HHS Public Access

Author manuscript

Methods Mol Biol. Author manuscript; available in PMC 2021 October 28.

Published in final edited form as:

Methods Mol Biol. 2020 ; 2138: 175–183. doi:10.1007/978-1-0716-0471-7_10.

Exploiting Plug-and-Play Electrochemical Biosensors to Determine the Role of FGF19 in Sorafenib-Mediated Superoxide and Nitric Oxide Production in Hepatocellular Carcinoma Cells

Lixia Gao[1,2], **Yong Teng**[1,3,4]

[1]Department of Oral Biology and Diagnostic Sciences, Dental College of Georgia, Augusta University, Augusta, USA

[2]Chongqing University of Arts and Sciences, Chongqing, People's Republic of China

[3]Georgia Cancer Center, Department of Biochemistry and Molecular Biology, Medical College of Georgia, Augusta University, Augusta, USA

[4]Department of Medical Laboratory, Imaging and Radiologic Sciences, College of Allied Health, Augusta University, Augusta, USA

Abstract

Electrochemical biosensors provide rapid, selective, and sensitive diagnostic platforms for detecting and monitoring biochemical processes in living systems in vivo and in vitro, and have been widely applied in various fields of biology and medicine. Sorafenib is a multi-kinase inhibitor used as a standard therapy for advanced hepatocellular carcinoma (HCC). However, the molecular basis for sorafenib resistance in HCC remains elusive. Recently, we developed new protocols for an electrochemical biosensor and applied these to monitor the levels of superoxide and nitric oxide produced in HCC cells, in the presence or absence of sorafenib. We also employed electrochemical biosensor to determine the release of profiles of superoxide and nitric oxide in sorafenib-treated HCC cells under the influence of fibroblast growth factor 19 expression levels. Here we present protocols to highlight the utility of electrochemical strategies in drug and gene studies.

Keywords

Electrochemical biosensors; Sorafenib; FGF19; Superoxide; Nitric oxide

1 Introduction

Biosensor-related research has experienced explosive growth over the last two decades and several methods have been successfully used to immobilize biological recognition molecules onto sensing surfaces with full functionality in biosensor-binding assays, such as enzyme-based electrochemical biosensors [1]. By converting a biological response into an electrical signal, electrochemical biosensors provide an attractive means to determine the content of biological samples or drugs through detecting and monitoring biochemical processes in

living systems upon physiological or pathological changes [1]. Details of electrochemical detection can be found in our review paper published in 2016 [1]. These electroanalytical methods generally require a three-electrode setup (working, counter, reference) with a potentiostat (Fig. 1). Electrochemical biosensors may be useful for drug-based and genetic studies through advances in quantification of biological or biochemical processes in a variety of biomedical and biotechnological applications in a cost- and time-effective manner.

Superoxide (O_2•−) and nitric oxide (NO) are the major free radicals and important signaling molecules that contribute to the pathogenesis of many diseases, including Alzheimer's disease, myocardial infarction, and cancer. It is noteworthy that O_2•− and NO can react with each other to produce significant amounts of a more oxidatively-active molecule called the peroxynitrite anion (ONOO−). This molecule causes deoxyribonucleic acid (DNA) fragmentation and lipid oxidation. Thus, there is a need to develop a method to monitor release of O_2•− and NO in cells in order to evaluate oxidative stress.

Fibroblast growth factor 19 (FGF19) is a metabolic regulator gene that belongs to the hormone-like FGF family of signal molecules, and has activity as an ileum-derived postprandial hormone [2–4]. FGF19 regulates hepatic bile acid levels through modulation of bile acid synthesis when it binds to the specific receptor FGFR4 [5]. FGF19 has been identified as an oncogenic driver in hepatocellular carcinoma (HCC) cells, and our previous studies have demonstrated that the FGF19/FGFR4 signaling contributes to the resistance of these cells to sorafenib [6, 7]. By employing electrochemical biosensors, we revealed that over-expression of FGF19 abrogated the sorafenib-induced increase in the intracellular levels of O_2•− and NO in HCC cells, leading to apoptosis resistance. These results provide a critical rationale for targeting the FGF19 signaling axis in patients with sorafenib-resistant HCC.

Here, we present new protocols for detecting the intracellular levels of O_2•− and NO using electrochemical biosensors.

2 Materials (*See* Note 1)

2.1 Synthesis of O_2•− Electrochemical Sensor

1. Deoxyribonucleic acid (DNA), low molecular weight from salmon sperm (*see* Note 2).
2. 0.1 M $MnSO_4$.
3. 0.1 M K_3PO_4.
4. Superoxide dismutase (SOD).
5. 0.5 mg/mL multi-walled carbon nanotube (CNT) (Sigma-Aldrich, St. Louis, MO, USA) (*see* Note 2).

The protocol has been optimized for use with this drug. The same drug from other suppliers will work but optimization may be required.

2. The protocol has been optimized for DNA and CNT and this product yields the best performance.

6. 5% Nafion® 117 solution (Sigma-Aldrich, St. Louis, MO, USA).
7. 0.01 M phosphate-buffered saline (PBS).
8. 15 mg/mL graphene oxide.
9. 0.1 M KO_2.

2.2 Synthesis of NO Electrochemical Sensor

1. 0.4 g poly-vinylpyrrolidone (PVP).
2. 0.434 g $Ce(NO_3)3•6H_2O$.
3. 3 mM NaOH.
4. 1 mM hemoglobin.

2.3 Polishing of Glassy Carbon Electrode

1. 0.3 and 0.05 mm alumina powder (ChenHua Instruments, Shanghai, China).
2. 0.1 M KCL.
3. 5 mM $K_3Fe(CN)_6$.
4. 5 mM $K_4[Fe(CN)_6]•3H_2O$.

2.4 Regents

1. HCC cells MHCC97L (ATCC, Rockville, MD, USA).
2. Sorafenib tosylate (Selleckchem; Houston, TX, USA).
3. Complete growth medium: 90% Gibco® Dulbecco's modified Eagle's medium (DMEM), containing 10% fetal bovine serum (FBS).
4. 0.25% trypsin-ethylenediaminetetraacetic acid (Trypsin-EDTA).
5. 0.01 M 3-(*N*-morpholino) propane sulfonic acid (MOPS) buffer (pH 7.2).
6. Dimethyl sulfoxide (DMSO).

2.5 *Equipment (*See Note 3)

1. Cyclic voltammetry (CV) potentiostat.
2. CHI760E electrochemical detector, glassy carbon electrode (d = 3 mm) (ChenHua Instruments).
3. $Hg/HgCl_2$/KCl reference electrode (ChenHua Instruments, Shanghai, China).
4. A platinum wire counter electrode (ChenHua Instruments, Shanghai, China).
5. Teflon-lined autoclave.

[3]There are no strict restrictions on the instruments used in this experiment and products of other companies can be used if they have corresponding functions.

3 Methods

3.1 Cell Culture

1. Remove the cryovial containing the frozen MHCC97L cells from liquid nitrogen storage and immediately place it into a 37 °C water bath.
2. Quickly thaw MHCC97L cells (<1 min) by gently swirling the vial in the 37 °C water bath until there is just a small bit of ice left in the vial.
3. Transfer the desired amount of pre-warmed complete growth medium (90% DMEM+10%FBS) drop-wise into the centrifuge tube containing the thawed cells.
4. Centrifuge the cell suspension at 200 × *g* for 5 min.
5. After the centrifugation, aseptically decant the supernatant without disturbing the cell pellet.
6. Gently resuspend cells in complete growth medium and let them grow to reach a confluence of 90–100%.

3.2 Preparation of O_2•− Electrochemical Biosensor (Fig. 2a)

1. Add 2.1 mg DNA into 1 mL 0.1 M $MnSO_4$ with constant stirring at 60 °C (*see* Note 4).
2. After 10 min, add 9 mL 0.1 M K_3PO_4 with stirring until the mixture becomes transparent (*see* Note 5).
3. Collect pellets of DNA@$Mn_3(PO_4)_2$ composites by centrifugation at 9000 × *g* for 10 min at 4 °C (*see* Note 6).
4. Dilute DNA@$Mn_3(PO_4)_2$ nanocomposite with 2 mL deionized water for subsequent experiments.
5. Maintain in a 4 °C refrigerator (*see* Note 7).
6. Drip 5 μL 0.5 mg/mL^{-1} CNT solution and drip on a polished glassy carbon electrode to dry under room temperature.
7. Drop-cast 5 μL DNA@$Mn_3(PO_4)_2$ mixture on the above electrode.
8. Calibrate O_2•− electrochemical sensors and detect the O_2•− level from cell release (*see* Note 8).

4. This protocol has been optimized for these experimental conditions. Other experimental methods need to be optimized.
5. We have optimized the reaction time and synthesis of the nanocomposites requires approximately 1 h. Therefore, when the reaction has been underway for this time, attention should be paid to whether or not the reactant solution becomes transparent. The reaction beaker should be placed in a water bath for heating and stirring.
6. This protocol has been optimized for the centrifugation time, strength and temperature.
7. Low temperature preservation is beneficial to the stability of the material performance, prolonging its service life.
8. Electrochemical sensor calibration is the only method to detect its sensitivity and detection limit and it is also a mark of successful sensor preparation. Therefore, this step is important in the process of constructing the electrochemical sensor.

3.3 Preparation of a NO Electrochemical Biosensor (Fig. 3a)

1. Dissolve 0.9 g PVP, 0.4 g $Ce(NO_3)3•6H_2O$ and 500 mL 15 mg/mL graphene oxide solution in 30 mL deionized water.
2. Stir 30 min at room temperature (*see* Note 9).
3. Transfer the mixture into the autoclave and heat at 180 °C 24 h (*see* Note 10).
4. Collect the obtained precipitate by centrifugation at 10,000 × *g* for 10 min at 4 °C.
5. Wash three times with ethanol and deionized water (*see* Note 6).
6. Dry the rGO/CeO_2 composites in an oven at 70 °C for 3 h (*see* Note 10).
7. Dissolve rGO/CeO_2 nanocomposites to 10 mg/mL in deionized water (*see* Note 11).
8. Sonicate rGO/CeO_2 solution 1 min before modification of the electrode (*see* Note 12).
9. Using the pipette, drain 5 μL rGO/CeO_2 nanocomposite solution and drip onto the polished glassy carbon electrode.
10. Dry at room temperature.
11. Calibrate NO electrochemical sensors and detect NO levelsfrom cell release (*see* Note 8).

3.4 Detection of Intracellular $O_2•−$ Levels in HCC Cells

1. Use the CV potentiostat to monitor intracellular $O_2•−$ generation on the electrochemical station (Fig. 2b, c).
2. Scan over a potential range of −0.25−0.85 V at 50 mV/s for $O_2•−$ electrochemical sensors (*see* Note 13).
3. Detect concentration changes of $O_2•−$ at 0.7 V by the amperometric response of $DNA@Mn_3(PO_4)_2$/CNT electrode (*see* Note 13).
4. Detect $O_2•−$ levels in MHCC97L cells with or without FGF19 over-expression in the presence of sorafenib using the electrochemical sensor (*see* Note 14).
5. Record peak current at 0.7 V.
6. Calculate the concentration of $O_2•−$ (Fig. 2d) (*see* Note 15).

---

9. We have optimized the stirring time and found that 30 min gives optimal results.
10. The temperature and time have been optimized to obtain the best experimental results.
11. The electrochemical sensor sensitivity and detection line are optimal at this concentration.
12. This sonication time has been optimized to obtain the best experimental results.
13. $DNA@Mn_3(PO4)_2$/CNT nanocomposites have a characteristic current peak over the range of 0.25–0.85 V. This has been optimized from our previous work.
14. Full-length human FGF19 cDNA was cloned into the pcDNA3.1(+) expression vector (Life Technologies, Carlsbad, CA, USA) and then transfected into MHCC97L cells.
15. Calculate the current change value of $O_2•−$ from cells with FGF19 over-expression (FGF19 O/E) with reference to the current value of cells without FGF19 over-expression (EV).

3.5 Detection of Intracellular NO Levels in HCC Cells

1. Use the CV potentiostat to monitor intracellular NO generation on the electrochemical station (Fig. 3b, c) (*see* Note 13).
2. Scan rGO/CeO_2 nanocomposites over 0.4–1.1 V at 50 mV/ s for NO electrochemical sensors (*see* Note 13).
3. Detect concentration changes of NO at 0.85 V by the amperometric response of the rGO/CeO_2 electrode (*see* Note 13).
4. Detect NO levels in MHCC97L cells with or without FGF19 over-expression in the presence of sorafenib using the electrochemical sensor (*see* Note 14).
5. Record the peak current at the 0.7 V and calculate the concentration of $NO^{\bullet-}$ (Fig. 3d) (*see* Note 16).

Acknowledgments

This research was supported by NIH grant R03DE028387 and R01DE028351 (to Y.T.).

References

1. Gao L, Teng Y (2016) Exploiting plug-and-play electrochemistry for drug discovery. Future Med Chem 8(5):567–577 [PubMed: 27079543]
2. Teng Y, Zhao H, Gao L, Zhang W, Shull AY, Shay C (2017) FGF19 protects hepatocellular carcinoma cells against endoplasmic reticulum stress via activation of FGFR4-GSK3beta-Nrf2 signaling. Cancer Res 77(22):6215–6225 [PubMed: 28951455]
3. Lang L, Shull AY, Teng Y (2019) Interrupting the FGF19-FGFR4 axis to therapeutically disrupt cancer progression. Curr Cancer Drug Targets 19(1):17–25 [PubMed: 29557750]
4. Zhao X, Xu F, Dominguez NP, Xiong Y, Xiong Z, Peng H et al. (2018) FGFR4 provides the conduit to facilitate FGF19 signaling in breast cancer progression. Mol Carcinog 57 (11):1616–1625 [PubMed: 30074276]
5. Lang L, Teng Y (2019) Fibroblast growth factor receptor 4 targeting in cancer: new insights into mechanisms and therapeutic strategies. Cell 8 (1):pii: E31. 10.3390/cells8010031
6. Gao L, Wang X, Tang Y, Huang S, Hu CA, Teng Y (2017) FGF19/FGFR4 signaling contributes to the resistance of hepatocellular carcinoma to sorafenib. J Exp Clin Cancer Res 36(1):8. 10.1186/s13046-016-0478-9 [PubMed: 28069043]
7. Gao L, Shay C, Lv F, Wang X, Teng Y (2018) Implications of FGF19 on sorafenib-mediated nitric oxide production in hepatocellular carcinoma cells—a short report. Cell Oncol (Dordr) 41(1):85–91 [PubMed: 28983785]

16. Calculate the current change value of $O_2^{\bullet-}$ from cells with FGF19 over-expression (FGF19 O/E) with reference to the current value of cells without FGF19 over-expression (EV).

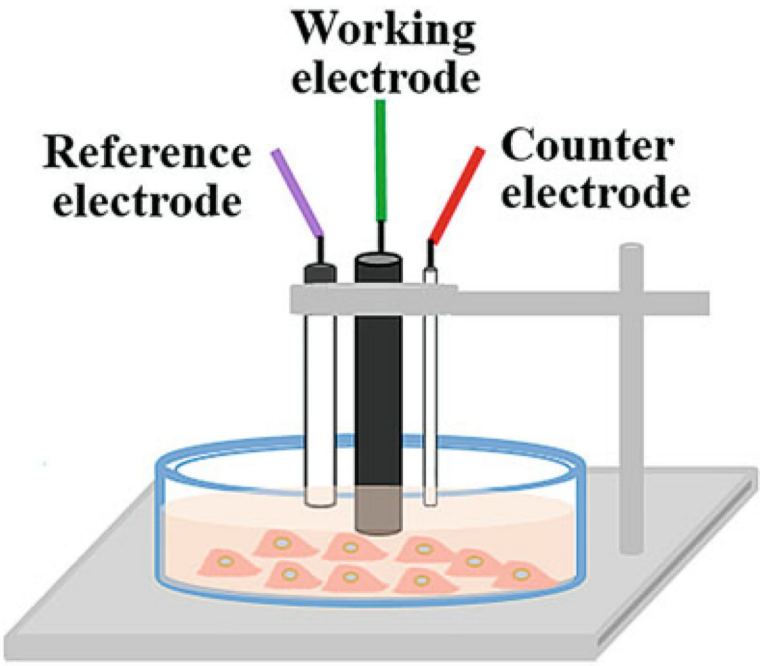

Fig. 1.
Schematic diagram of classic three-electrode electrochemical biosensor detection system

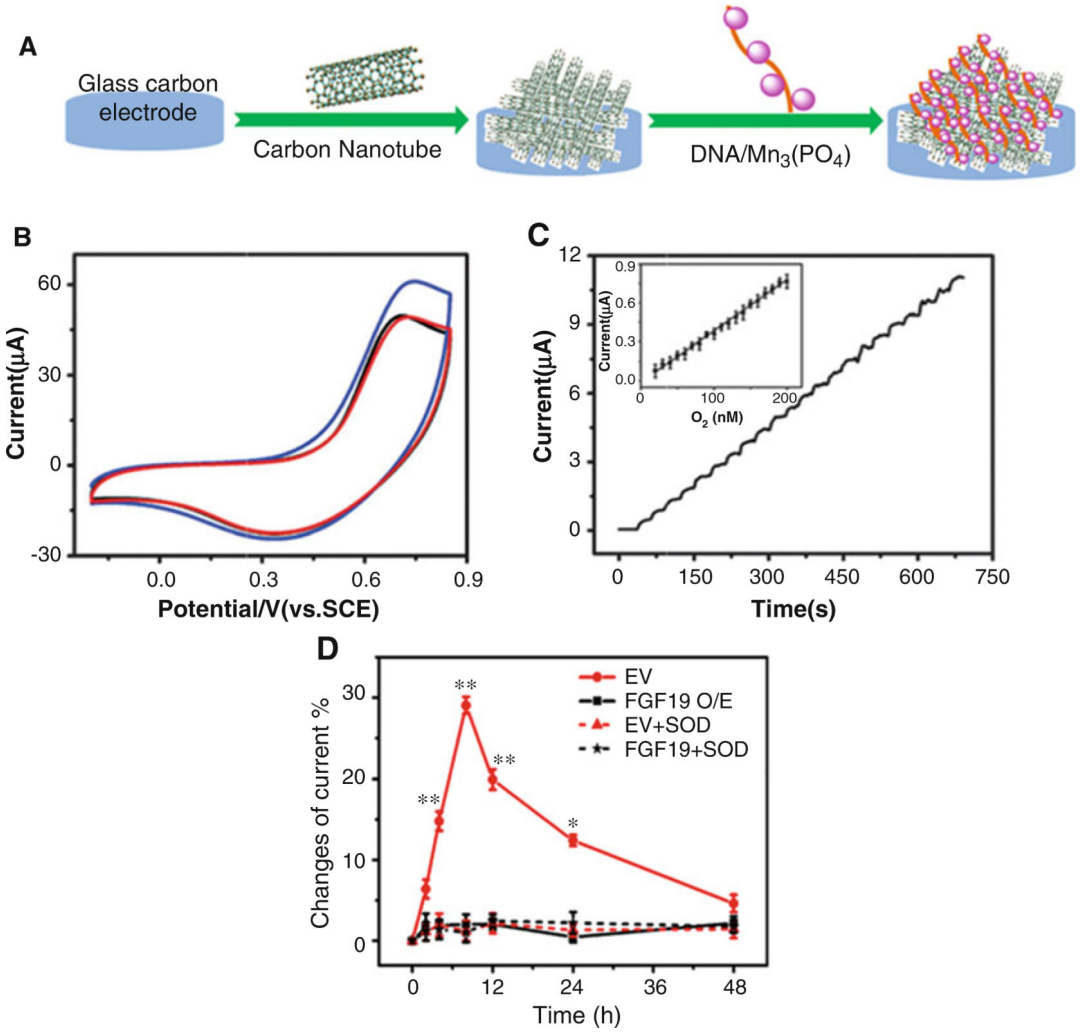

Fig. 2.

The use of DNA@$Mn_3(PO_4)_2$/CNT electrochemical biosensor to determine the O_2•− level released from MHCC97L cells with different treatments. (**a**) Schematic diagram of synthesis of DNA@$Mn_3(PO_4)_2$/CNT nanocomposite. (**b**) Cyclic voltammetry curves measured in PBS (black line), PBS + 100 nM KO_2 (blue line) and PBS + 100 nM KO_2 + superoxide dismutase (red line). (**c**) Amperometric response (*i–t* curve) and calibration curve for serial concentrations of KO_2. (**d**) FGF19 overexpression protects HCC cells against sorafenib. O_2•− generation level was determined by an electrochemical biosensor

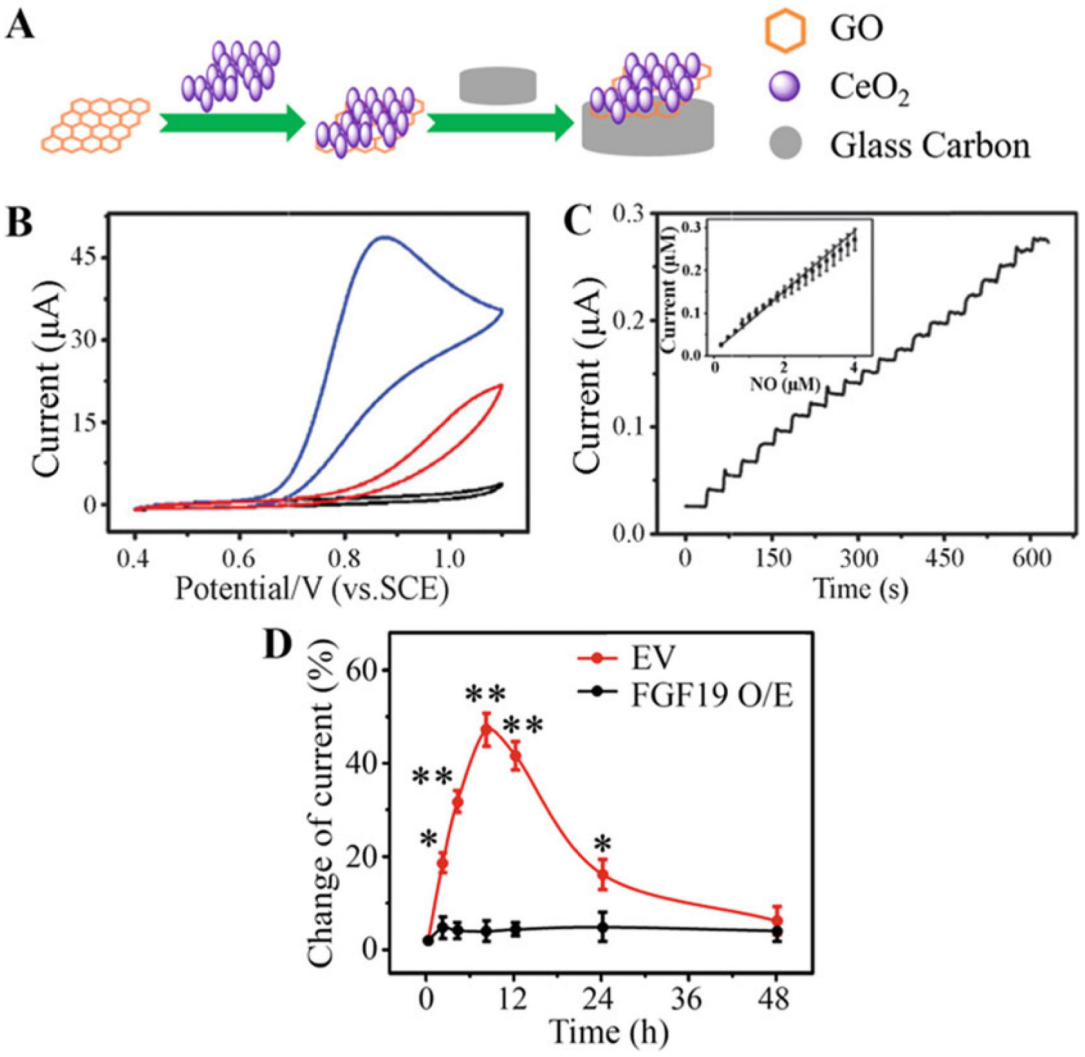

Fig. 3.

The use of rGO/CeO_2 electrochemical biosensor to determine NO levels released from MHCC97L cells with different treatments. (**a**) Schematic diagram of synthesis of rGO/CeO_2 nanocomposite. (**b**) Cyclic voltammetry curves measured in PBS (black line), PBS + 250 μM NO (blue line) and PBS + 250 μM NO + hemoglobin (redline). (**c**) Amperometric response (*i–t* curve) and calibration curve for a serial concentration of NO. (**d**) FGF19 over-expression protects HCC cells against sorafenib. NO generation level was determined by an electrochemical biosensor